

Deep search for gamma-ray emission from the accreting X-ray pulsar 1A 0535+262

X. HOU,^{1,2} W. ZHANG,^{3,4} D.F. TORRES,^{3,4,5} L. JI,⁶ AND J. LI^{7,8}

¹*Yunnan Observatories, Chinese Academy of Sciences, Kunming 650216, China*

²*Key Laboratory for the Structure and Evolution of Celestial Objects, Chinese Academy of Sciences, Kunming 650216, China*

³*Institute of Space Sciences (ICE, CSIC), Campus UAB, 08193 Barcelona, Spain*

⁴*Institut d'Estudis Espacials de Catalunya (IEEC), 08034 Barcelona, Spain*

⁵*Institució Catalana de Recerca i Estudis Avançats (ICREA), E-08010 Barcelona, Spain*

⁶*School of Physics and Astronomy, Sun Yat-Sen University, Zhuhai 519082, China*

⁷*CAS Key Laboratory for Research in Galaxies and Cosmology, Department of Astronomy, University of Science and Technology of China, Hefei, China*

⁸*School of Astronomy and Space Science, University of Science and Technology of China, Hefei, China*

(Accepted for publication in ApJ)

ABSTRACT

Binary systems are a well-established subclass of gamma-ray sources. The high mass X-ray binary pulsar 1A 0535+262 has been considered to be a possible gamma-ray emitter for a long time, although former gamma-ray searches using *Fermi*-LAT and VERITAS data resulted in upper limits only. We aim at a deep search for gamma-ray emission and pulsations from 1A 0535+262 using more than 13 years of *Fermi*-LAT data. The analysis was performed for both the whole *Fermi*-LAT data set, as well as for the X-ray outbursts that 1A 0535+262 has experienced since the launch of *Fermi*. Various X-ray observations have been used to generate the ephemeris for the pulsation search. We also investigate the long-term gamma-ray flux variability and perform orbital phase-resolved analysis for the outbursts. We did not detect any steady or pulsed gamma-ray emission from 1A 0535+262 during the whole *Fermi*-LAT mission span or its X-ray outbursts. We thus derived the deepest gamma-ray luminosity upper limits to date at the 95% confidence level to be around $(2.3\text{--}4.7)\times 10^{32}$ erg s⁻¹ depending on different spectral indices assumed, which results in a ratio of L_γ to L_X (2–150 keV) being $(1.9\text{--}3.9)\times 10^{-6}$.

Keywords: stars: neutron — X-rays: binaries — Gamma rays

1. INTRODUCTION

Among the various gamma-ray sources detected in the MeV/GeV and/or even the TeV band, binary systems are a well-established subclass, although their number is yet small. Interestingly, despite their

small number, several varieties of binaries exist with different gamma-ray emission mechanisms. For a recent review, see [Dubus \(2015\)](#). First, *Fermi*-LAT has detected gamma-ray binaries themselves, usually defined as a subclass of high mass X-ray binaries (HMXBs) with O or B companion star, with two main features: they emit modulated gamma rays peaking above 1 MeV and present orbital variability at all frequencies. The spectral energy distribution is usually thought to be powered by the pulsar/stellar wind interaction, although so far the central compact object has been associated to known pulsars only in three cases: PSR B1259-63/LS 2883 (see [Abdalla et al. 2020](#); [Chernyakova et al. 2020](#), and references therein), PSR J2032+4127/MT91 213 (see [Coe et al. 2019](#), and references therein), and the recent identification of LS I +61 303 ([Weng et al. 2022](#)).

Recycled pulsars in binaries, called redbacks & black widow systems, are tight (orbital periods less than a day), low mass ($< 0.1M_{\odot}$) gamma-ray binaries with a main sequence degenerate companion. In these systems the pulsar wind is ablating the companion star, leading to eclipses, radio variability, X-ray/radio anti-correlation, and pulsar nulling (see, e.g., [Bogdanov et al. 2018](#)). Transitional pulsars are special among these systems, since they exhibit two different states (accretion and rotation powered) which may interchange in a matter of weeks and persist for years (see e.g., [Archibald et al. 2009](#); [Papitto et al. 2013](#); [de Martino et al. 2015](#)). These state changes produce significant gamma-ray variability ([Stappers et al. 2014](#); [Torres et al. 2017](#)).

Other *Fermi*-LAT detected binaries include microquasars, for which the gamma rays seem to be associated with a relativistic jet. Notable examples are Cyg X-1 (see e.g., [Albert et al. 2007](#); [Zanin et al. 2016](#); [Zdziarski et al. 2017](#)) and Cyg X-3 (see e.g., [Abdo et al. 2009](#); [Tavani et al. 2009](#); [Zdziarski et al. 2018](#); [SinitSYna & SinitSYna 2019](#)). The microquasar SS 433, whose central object is still undetected, was unexpectedly found to produce gamma rays far from the jet ([Abeysekara et al. 2018](#); [Rasul et al. 2019](#); [Xing et al. 2019](#); [Fang et al. 2020](#)) with a GeV source showing variability with the precession period of the system ([Li et al. 2020](#)).

Finally, one finds the accreting millisecond pulsar SAX J1808.4–3658 ([de Oña Wilhelmi et al. 2016](#)): a “*bona fide*” accreting system apparently emitting gamma rays, although yet not significantly. This is the only such system for which a gamma-ray detection was hinted so far. Putting upper limits on accreting sources or detecting them is a must to understand the different variety.

1A 0535+262 is one of the best studied HMXB accreting pulsars. It was discovered in 1975 by the Rotation Modulation Collimator on *Ariel V*, with a pulsation period of 104 s ([Rosenberg et al. 1975](#)). The compact object in the system is a highly magnetized neutron star which accretes mass from the O9.7IIIe companion star ([Steele et al. 1998](#)). The orbital period of the system is ~ 111 days ([Coe et al. 2006](#)) and the eccentricity of the orbit is $e = 0.47 \pm 0.02$ ([Finger et al. 1996](#)). 1A 0535+262 is relatively close to Earth with a distance of 1.8 ± 0.1 kpc, as measured by *Gaia* ([Bailer-Jones et al. 2018](#)). Since its discovery, 1A 0535+262 has exhibited different X-ray outbursts with peak flux ranging from ~ 100 mCrab to ~ 12.5 Crab. In particular, three giant X-ray outbursts were detected since the launch of the *Fermi* satellite: in 2009 December ([Acciari et al. 2011](#)), 2011 February ([Sartore et al. 2015](#)) and 2020 November ([Kong et al. 2022](#); [Mandal & Pal 2022](#), and references therein). Figure 1 shows the long-term light curves of 1A 0535+262 in different energy bands obtained from the *Swift*/BAT and *MAXI*/GSC Broadband Transient Monitor¹. There was also a double-peaked outburst ([Caballero et al. 2013](#)) just prior to the 2009 giant one, which is,

¹ http://sakamotoagu.mydns.jp/bat_gsc_trans_mon/web_lc/1_Day.php?name=1A_0535+262

however, not included in the monitor database. VLA observations during the 2020 outburst revealed non-thermal radio emission from the source position (van den Eijnden et al. 2020).

1A 0535+262 was earlier associated with the EGRET unidentified gamma-ray source 3EG J0542+2610 (Romero et al. 2001) and thus has long been considered as a high-energy (HE; $E > 100$ MeV) and very-high-energy (VHE; $E > 100$ GeV) emitter candidate. The first gamma-ray search for 1A 0535+262 dates back to more than 10 years, during its giant 2009 outburst. On that occasion, the X-ray outburst in December of 2009 triggered VHE VERITAS observations. Only upper limits have been derived (Acciari et al. 2011). These authors also did a search for HE gamma-ray emission from 1A 0535+262 with *Fermi*-LAT in a period spanning the onset of the X-ray outburst to the successive apastron of the pulsar (2009 November 30 to 2010 February 22). No significant GeV excess was seen and a flux upper limit of $F(> 0.2 \text{ GeV}) < 1.9 \times 10^{-8} \text{ photons cm}^{-2} \text{ s}^{-1}$ at 99% confidence level was imposed. Recently, Lundy (2021) updated the VERITAS VHE search for 1A 0535+262 during its 2020 giant outburst. Again, only upper limits have been obtained. Also, Harvey et al. (2022) used 12.5 years LAT data to search for gamma-ray emission from 1A 0535+262. They claimed a marginal persistent gamma-ray excess (3.5σ) at the position of the source and found that the gamma-ray activity may be correlated with the X-ray outbursts. In addition, they found that essentially all of the gamma-ray excess is concentrated in the orbital phase bin preceding periastron, thus providing evidence of the gamma-ray excess originating from this binary system. If real, these hints are relevant, and thus can help to get insights to the particle acceleration and emission process during the accretion.

In this work, we analyze the three giant outbursts, in 2009, 2011 and 2020, and the previous double-peaked outburst of 1A 0535+262. The time span of each outburst was defined by investigating the X-ray light curves presented in the literature (Acciari et al. 2011; Sartore et al. 2015; Mandal & Pal 2022; Kong et al. 2022). We perform a deep search for gamma-ray emission and pulsations from 1A 0535+262 using more than 13 years of *Fermi*-LAT data and the latest 12-year source catalog. We use the latest Instrument Response Functions (IRFs) and background diffuse models. Our work therefore extends the result presented in Harvey et al. (2022). The paper is organized as follows: we describe the data analysis procedure and results in Section 2, and discuss our findings in Section 3. We finally conclude in Section 4.

2. DATA ANALYSIS AND RESULTS

2.1. Timing solutions

For the 2009 double-peaked and giant outbursts, we adopted the spin measurements and the orbital ephemeris of 1A 0535+262 from the *Fermi*/GBM monitoring². We used a polynomial function to describe the spin evolution approximately. For the 2011 outburst, we used the timing solution reported in Sartore et al. (2015) derived using *INTEGRAL* observations. For the recent 2020 outburst, thanks to the extensive coverage of *Insight*-HXMT observations (Wang et al. 2022), we used the phase-connection technique (Deeter et al. 1981) to determine the spin evolution accurately. In practice, for each 1000 s segment we folded background-subtracted light curves in the energy range of 25–80 keV, for which the pulse profile shape is relatively stable. The 1000 s was chosen because this is the typical interval for *Insight*-HXMT’s good time. The time-of-arrival (TOA) of each segment was estimated

² <https://gammaray.nsstc.nasa.gov/gbm/science/pulsars/lightcurves/a0535.html>

by cross-correlating these pulse profiles with an averaged template. Then the spin evolution was determined by using the software TEMPO2 (Hobbs et al. 2006). We summarize the timing solutions for different outbursts used in the following pulsation search (Section 2.5) in Table 2.

2.2. *Fermi-LAT data set and reduction*

We used the Pass 8 data set (Atwood et al. 2013; Bruel et al. 2018) available at the *Fermi* Science Support Center (FSSC)³. This spans 166 months, from 2008 August 4 to 2022 June 9, with reconstructed energy in the range 0.1–300 GeV. We selected SOURCE class events (Front and Back) with a zenith angle smaller than 90° to avoid the Earth limb contamination. The events were further filtered based on the criteria ‘‘DATA_QUAL>0 && LAT_CONFIG==1’’ to get the good time intervals in which the satellite was working in standard data taking mode and the data quality was good. We did not apply a Region of Interest (ROI)-based zenith angle cut⁴. The data set was centered at 1A 0535+262 with coordinates $(\alpha, \delta) = (84^{\circ}.7274, 26^{\circ}.3158)$, with a radius of 10°. The coordinates of 1A 0535+262 were taken from the SIMBAD⁵ database and in the J2000 frame. The analysis was performed using the P8R3_SOURCE_V3 IRFs and the latest Fermitools⁶ (v2.2.0) available at the FSSC.

2.3. *Fermi-LAT spectral analysis*

In the spectral analysis, the latest 4FGL-DR3⁷ (gll_psc_v30.fit) (Fermi-LAT collaboration 2022) sources within a 20° circle around 1A 0535+262 were included to build a complete spatial and spectral source model. We also included the latest Galactic interstellar emission model, ‘‘gll_iem_v07.fits’’, as well as the isotropic emission spectrum ‘‘iso_P8R3_SOURCE_V3_v1.txt’’, with the latter taking into account the extragalactic emission and the residual instrumental background⁸. Both the normalizations and spectral indices of sources within 5° around 1A 0535+262 were set free to vary except for 4FGL J0534.5+2201i, which is recommended to be fixed to account for the Inverse Compton Scattering component of the Crab Nebula. Extended sources were modeled using the 12-year templates. Since the closest source in the model is $\sim 1.6^{\circ}$ away from 1A 0535+262, we added 1A 0535+262 manually in the model as a point source with a simple Power Law spectral model. This allows us to check whether the addition of such source is significant.

Model fitting was performed in a $14^{\circ} \times 14^{\circ}$ ROI using the maximum likelihood method (Mattox et al. 1996). We followed the binned likelihood procedure outlined in the FSSC using a $0^{\circ}.1 \times 0^{\circ}.1$ pixel size and thirty logarithmic energy bins over 0.1–300 GeV. Two extra energy bins have been added to take into account the energy dispersion except for the isotropic component. The significance of a given source in the model is characterized by the Test Statistic (TS), which is expressed as $TS = 2(\log \mathcal{L} - \log \mathcal{L}_0)$, where $\log \mathcal{L}$ and $\log \mathcal{L}_0$ are the logarithms of the maximum likelihood of the complete source model and of the background model (i.e. the source model without the given source included), respectively.

We first performed a global binned likelihood fit to the whole data set by fixing the spectral index of 1A 0535+262 to 2, 2.3 and 3, respectively. Such spectral indices are chosen to represent possible emission mechanisms. At the same flux level, if the source were to emit a hard spectrum (as the

³ <http://fermi.gsfc.nasa.gov/ssc/>

⁴ https://fermi.gsfc.nasa.gov/ssc/data/analysis/scitools/data_preparation.html

⁵ <http://simbad.u-strasbg.fr/simbad/>

⁶ <https://fermi.gsfc.nasa.gov/ssc/data/analysis/software/>

⁷ https://fermi.gsfc.nasa.gov/ssc/data/access/lat/12yr_catalog/

⁸ <https://fermi.gsfc.nasa.gov/ssc/data/access/lat/BackgroundModels.html>

assumed 2) across the *Fermi*-LAT energy regime, it should be easier to detect it due to the diminishing background at higher energies. Then, using the best-fit source model from the whole data set fit, we performed binned likelihood fits to the different X-ray outbursts that 1A 0535+262 has experienced in the past, following the same fitting setup and procedure as for the whole data set. To increase the detection possibility and statistics, we also stacked all the outbursts together to perform the fit. 1A 0535+262 was not detected in any of these cases and we therefore computed a 95% confidence level energy flux upper limit accordingly. The fitting results are presented in Table 1.

2.4. Gamma-ray variability

We performed two different types of variability analysis for 1A 0535+262. First, to investigate the long-term gamma-ray flux variability, we computed light curves with a 180-day binning as in Harvey et al. (2022) in the energy range of 0.1–300 GeV for all spectral indices used in the spectral analysis (Figure 1). The full data best-fit source model was used as an input for each time bin and the normalizations of sources within 3° around 1A 0535+262 were set free to vary. Upper limits at 95% confidence level were calculated when 1A 0535+262 had $TS < 4$ in a given time bin. We did not see any significant detection in all the time bins when fixing the spectral index to 2 or 2.3. For the light curve with index fixed to 3, there are two bins with TS being about 10 and 20, corresponding to approximately 3σ and 4σ . However, these two bins correspond to the period where its X-ray emission was faint according to the X-ray monitoring of 1A 0535+262 (Figure 1). Thus, we conclude that no correlation between gamma-ray and X-ray was observed, contrary to what Harvey et al. (2022) has claimed. Furthermore, the variability significance was computed following the same method used in Acero et al. (2015). Only the light curve with index fixed to 3 has a non-negligible significance (1.7σ for 27 degrees of freedom), but this is far from declaring a significant variability, which requires usually a significance of at least 3σ . Any gamma-ray emission is thus consistent with being steady on a timescale of a few months based on our analysis.

Since gamma-ray binaries usually exhibit orbital flux variability, we also computed the orbital flux for 1A 0535+262 with 10 bins per orbit and calculated upper limits at 95% confidence level when 1A 0535+262 had $TS < 4$ in a given orbital bin, as was done in Harvey et al. (2022). Similar to the long-term light curve, the full data best-fit source model was used as an input for each orbital bin and the spectral index was fixed to 2, 2.3 and 3, respectively. No significant orbital variability was observed. The orbital light curves are shown in Figure 2.

2.5. Gamma-ray pulsation search

We performed a pulsation search using reconstructed LAT photons within 1° of 1A 0535+262 in the energy range of 0.1–300 GeV. The signal significance was qualified using the weighted H-test developed by Kerr (2011), which is based on the original one proposed by de Jager et al. (1989):

$$H_{mw} = \max [Z_{iw}^2 - c \times (i - 1)], \quad 1 \leq i \leq m, \quad (1)$$

where

$$Z_{mw}^2 = \frac{2}{\sum_{i=1}^N w_i^2} \times \sum_{k=1}^m (\alpha_{wk}^2 + \beta_{wk}^2), \quad (2)$$

and

$$\alpha_{wk} = \sum_{i=1}^N w_i \cos(2\pi k \phi_i), \quad \beta_{wk} = \sum_{i=1}^N w_i \sin(2\pi k \phi_i). \quad (3)$$

Here, N is the total photon number, ϕ_i is the pulsar rotational phase and w_i is the photon weight, m is the maximum search harmonic and c is the offset for each successive harmonic. We used the standard value $c = 4$ and varied m in our analysis. We verified that taking the standard value $m = 20$ did not change the result.

We employed the Simple Weights method described in [Bruel \(2019\)](#) and [Smith et al. \(2019\)](#) to compute the weight for each photon. This is considered as a proxy for the probability that the photon comes from 1A 0535+262. Assuming that the target source is faint compared to the diffuse background and that the background emission is isotropic, for a photon with energy E (in MeV) and angular distance $\Delta\theta$ to the target source, the weight is:

$$w(E, \Delta\theta) = f(E) \times g(E, \Delta\theta), \quad (4)$$

where

$$f(E) = \exp(-2\log_{10}^2(E/E_{\text{ref}})) \quad (5)$$

is the weight at the pulsar position, which depends on the pulsar and background spectra and on the LAT's energy-dependent Point Spread Function (PSF). The geometrical factor $g(E, \Delta\theta)$ describes the angular distribution of the gamma-ray photons emitting from a point source and can be written as

$$g(E, \Delta\theta) = \left(1 + \frac{9\Delta\theta^2}{4\sigma_{\text{psf}}^2(E)}\right)^{-2}, \quad (6)$$

where

$$\sigma_{\text{psf}}(E) = \sqrt{p_0^2(E/100)^{-2p_1} + p_2^2} \quad (7)$$

is the PSF 68% containment angle with $p_0 = 5.445$, $p_1 = 0.848$ and $p_2 = 0.084$ for LAT P305 Pass 8 data ([Atwood et al. 2013](#)).

Defining the reference energy $E_{\text{ref}} = 10^{\mu_w}$, the H-test versus μ_w follows a Gaussian distribution ([Bruel 2019](#)). Thus, searching for pulsations means finding the maximum H-test by scanning over μ_w . After searching a thousand radio pulsars for possible gamma-ray emission, [Smith et al. \(2019\)](#) indicate that in most cases $\mu_w = 3.6$ is a good choice to yield a significant signal. We adopted this value in our pulsation search for 1A 0535+262. Considering that this value was found for non-accreting (and many isolated) radio pulsars that have a power law with an exponential cutoff (PLEC) spectrum ([Abdo et al. 2013](#)), and thus may not be appropriate for an accreting system that could have a different spectral shape, we also verified that scanning over μ_w to find the best value does not affect the result significantly. We used the ephemerides for different observations (Table 2) to phase-fold the gamma-ray photons of 1A 0535+262, restricting the pulsation search range to the validity of the corresponding ephemerides. However, no significant pulsation was detected during the individual outbursts. Although a signal of $\sim 1.5\sigma$ was hinted for the 2009 outburst, the significance is far from the LAT detection threshold of 4σ .

3. DISCUSSION

In general, we obtained very different results compared to [Harvey et al. \(2022\)](#). We had no detection of either persistent or transient or pulsed gamma-ray emission from 1A 0535+262. Although we have two time bins with $\text{TS} \sim 20$ and ~ 10 , they did not correspond to the X-ray outburst periods. Therefore, our result does not support their conclusion that the gamma-ray emission is correlated

with the X-ray outburst of the source and is mostly concentrated in specific orbital bins. Such difference may mainly come from the fitting procedure and whether or not considering the energy dispersion. We normally fitted the sources within 5° around 1A 0535+262 in the spectral fit and orbital flux variability study, and within 3° for the long-term light curves, while they fitted only 1° around 1A 0535+262. In addition, the spectral index was fixed to different values to account for possible emission mechanisms in our study, while they let the index free to vary. Actually, for the long-term variability, no detailed fitting procedure information was found in [Harvey et al. \(2022\)](#), making a detailed comparison difficult.

Unlike those cases when a detection is found from an astrophysical source, the possible reasons for a non-detection are essentially unlimited. Gamma-ray binary systems such as LS I +61 303 are radio sources, and their X-ray spectra contain a significant non-thermal component. Recently, radio pulsations were detected from this system ([Weng et al. 2022](#)). Thus, it is worth noting that LS I +61 303 is probably not a significantly accreting system, and thus it likely has a different acceleration and emission mechanism than that acting in 1A 0535+26, if there is any in the latter. On the other hand, in 1A 0535+262, the absence of a significant quiescent radio emission that could later be associated with non-thermal processes may simply indicate that leptons are not sufficiently accelerated there. This observation had earlier promoted hadronic models. From our results, though, we can also rule out hadronic production acting according to a mechanism originally proposed by [Cheng & Ruderman \(1991\)](#), where a proton beam accelerated in a magnetospheric electrostatic gap impacts the transient accretion disk. This model was applied to 1A 0535+262 by [Romero et al. \(2001\)](#), [Anchordoqui et al. \(2003\)](#) and [Orellana et al. \(2007\)](#). Particularly in the latter paper the theoretical flux prediction of 3.8×10^{-8} ph cm $^{-2}$ (derived by extrapolating the result of [Orellana et al. 2007](#)), i.e., a gamma-ray luminosity of about 10^{33} erg s $^{-1}$ at 0.3 TeV at the end of giant outbursts to the *Fermi*-LAT energy range (see [Acciari et al. 2011](#)) is above our limit which is $\sim(2.3-4.7) \times 10^{32}$ erg s $^{-1}$ by one order of magnitude (and should have been detected earlier on in the mission) depending on different spectral indices assumed. Taking the X-ray luminosity (2–150 keV) reported for the largest 2020 outburst ([Kong et al. 2021](#)) to be 1.2×10^{38} erg s $^{-1}$, the ratio of L_γ to L_X is then calculated to be $(1.9-3.9) \times 10^{-6}$.

It remains to be seen, of course, whether the flux was overestimated but the mechanism is still viable, or whether a longer integration might lead to low-flux quiescent emission or to an occasional detection. None of these possibilities has happened in the long integration time we have analyzed. At least with the current gamma-ray sensitivity, 1A 0535+262 is not a gamma-ray source. With our current limits, there appears to be no reasonable combination of the hadronic model parameters to still accommodate a persistent gamma-ray flux.

Another interpretation could simply be that none of the possible shocks in the system is energetic enough to produce sufficiently accelerated particles able to emit gamma-rays. Or that if they do, the radiation produced is absorbed due to the matter in the surroundings, see e.g., the discussion in [Orellana et al. \(2007\)](#). Regarding the latter, it would be reasonable to expect that any absorption would be quite variable. Thus if the emission is produced in the system at all, it would be unlikely that it is absorbed all the time. In addition, secondary electrons (and positrons) from the pair production process would generate gamma rays at MeV–GeV energies, (see e.g., [Bednarek 1997, 2006](#); [Sierpowska-Bartosik & Torres 2008](#)). These could be attenuated by X-ray photons, but probably not fully attenuated after the X-ray peak has passed.

Giant (or Type II) outbursts, though they are rare and unrelated to the orbital cadence, may have X-ray luminosities close to the Eddington limit. They are likely associated with the formation of a transient accretion disk. Recently, [van den Eijnden et al. \(2020\)](#) detected a radio counterpart during the 2020 outburst. This was the first time that a coupled increase in X-ray and radio flux was seen in 1A 0535+262 and shows that the radio emission may relate to the accretion state. This would be similar to the behaviour seen in the transient Be X-ray binary Swift J0243.6+6124 ([van den Eijnden et al. 2018](#)). [Bednarek \(2009a,b\)](#) proposed that it is possible that HMXBs produce gamma-ray emission during accretion periods. The possibility that particle acceleration can take place even when mass accretion is going on is supported by some observational results: the hinted gamma-ray emission from SAX J1808.4–3658 ([de Oña Wilhelmi et al. 2016](#)), the gamma-ray emission found from the sub-luminous state of the transitional pulsars (as quoted in the introduction) and interpreted as propeller emission (see e.g., [Papitto et al. 2014](#); [Papitto & Torres 2015](#)) or a mini pulsar wind nebula ([Papitto et al. \(2019\)](#), see also [Veledina et al. \(2019\)](#)) and finally, the discovery of optical and ultraviolet pulsed emission from the accreting millisecond pulsar SAX J1808.4–3658 ([Ambrosino et al. 2021](#)). However, the neutron star Eddington luminosity ($L_{\text{Edd}} \sim 1.8 \times 10^{38} \text{ erg s}^{-1}$) is many orders of magnitude above our upper limits, pointing to a very inefficient mechanism, if at play at all. Similarly to the case of other transients, for instance, the Be X-Ray Binary 4U 1036–56 (RX J1037.5–5647), which could be associated to *AGILE* transients, we cannot discard that a low level of gamma-ray flux is emitted at lower energies, below 100 MeV (see [Li et al. 2012](#), and in particular their figure 6 for an associated discussion). This remains to be tested with the advent of MeV missions such as AMEGO ([McEnery et al. 2019](#)), e-ASTROGAM ([de Angelis et al. 2018](#)), or COSI ([Beechert et al. 2022](#)).

4. CONCLUSIONS

We have searched for gamma-ray emission and pulsations from 1A 0535+262 using more than 13 years of *Fermi*-LAT data. Neither persistent nor transient nor pulsed gamma-ray emission has been detected significantly in our study for the whole data set or during the X-ray outbursts that 1A 0535+262 has experienced since the launch of the *Fermi* satellite. Upper limits on the luminosity at the 95% confidence level were derived to be around $(2.3\text{--}4.7) \times 10^{32} \text{ erg s}^{-1}$ depending on different spectral indices assumed, the deepest ones to date. The emission of 1A 0535+262 is considered to be consistent with being steady on a timescale of a few months. Although two time bins in the long-time light curve hint to have gamma-ray emission at roughly 3 and 4σ , they occurred when the source was faint in X-rays. Thus, no correlation between gamma-ray and X-ray activities was observed based on our result. In addition, we did not see any significant orbital gamma-ray variation. We conclude that 1A 0535+262 is not a gamma-ray emitter at the level of the current gamma-ray sensitivity.

ACKNOWLEDGMENTS

The *Fermi* LAT Collaboration acknowledges generous ongoing support from a number of agencies and institutes that have supported both the development and the operation of the LAT, as well as scientific data analysis. These include the National Aeronautics and Space Administration and the Department of Energy in the United States; the Commissariat à l’Energie Atomique and the Centre National de la Recherche Scientifique/Institut National de Physique Nucléaire et de Physique des Particules in France; the Agenzia Spaziale Italiana and the Istituto Nazionale di Fisica Nucleare in Italy; the Ministry of Education, Culture, Sports, Science and Technology (MEXT), High Energy Accelerator Research Organization (KEK), and Japan Aerospace Exploration Agency (JAXA) in Japan; and the K. A. Wallenberg Foundation, the Swedish Research Council, and the Swedish National Space Board in Sweden. Additional support for science analysis during the operations phase is gratefully acknowledged from the Istituto Nazionale di Astrofisica in Italy and the Centre National d’Études Spatiales in France.

This work was performed in part under DOE Contract DE-AC02-76SF00515. The authors are supported by the National Natural Science Foundation of China through grants U1938103, 12041303, 12173103, U2038101, 11733009. WZ and DFT work have been supported by the grant PID2021-124581OB-I00 funded by MCIN/AEI/10.13039/501100011033 and by the Spanish program Unidad de Excelencia María de Maeztu CEX2020-001058-M. DFT acknowledges as well USTC and the Chinese Academy of Sciences International Presidential Fellowship Initiative 2021VMA0001. This research has made use of the SIMBAD database, operated at CDS, Strasbourg, France.

REFERENCES

- Abdalla, H., Adam, R., Aharonian, F., et al. 2020, *A&A*, 633, A102, doi: [10.1051/0004-6361/201936621](https://doi.org/10.1051/0004-6361/201936621)
- Abdo, A. A., Ackermann, M., Ajello, M., et al. 2009, *Science*, 326, 1512, doi: [10.1126/science.1182174](https://doi.org/10.1126/science.1182174)
- Abdo, A. A., Ajello, M., Allafort, A., et al. 2013, *ApJS*, 208, 17, doi: [10.1088/0067-0049/208/2/17](https://doi.org/10.1088/0067-0049/208/2/17)
- Abeysekara, A. U., Albert, A., Alfaro, R., et al. 2018, *Nature*, 562, 82, doi: [10.1038/s41586-018-0565-5](https://doi.org/10.1038/s41586-018-0565-5)
- Acciari, V. A., Aliu, E., Araya, M., et al. 2011, *ApJ*, 733, 96, doi: [10.1088/0004-637X/733/2/96](https://doi.org/10.1088/0004-637X/733/2/96)
- Acero, F., Ackermann, M., Ajello, M., et al. 2015, *ApJS*, 218, 23, doi: [10.1088/0067-0049/218/2/23](https://doi.org/10.1088/0067-0049/218/2/23)
- Albert, J., Aliu, E., Anderhub, H., et al. 2007, *ApJL*, 665, L51, doi: [10.1086/521145](https://doi.org/10.1086/521145)
- Ambrosino, F., Miraval Zanon, A., Papitto, A., et al. 2021, *Nature Astronomy*, 5, 552, doi: [10.1038/s41550-021-01308-0](https://doi.org/10.1038/s41550-021-01308-0)
- Anchordoqui, L. A., Torres, D. F., McCauley, T. P., Romero, G. E., & Aharonian, F. A. 2003, *ApJ*, 589, 481, doi: [10.1086/374551](https://doi.org/10.1086/374551)
- Archibald, A. M., Stairs, I. H., Ransom, S. M., et al. 2009, *Science*, 324, 1411, doi: [10.1126/science.1172740](https://doi.org/10.1126/science.1172740)
- Atwood, W., Albert, A., Baldini, L., et al. 2013, *ArXiv e-prints*, <https://arxiv.org/abs/1303.3514>
- Bailer-Jones, C. A. L., Rybizki, J., Foesneau, M., Mantelet, G., & Andrae, R. 2018, *AJ*, 156, 58, doi: [10.3847/1538-3881/aacb21](https://doi.org/10.3847/1538-3881/aacb21)
- Bednarek, W. 1997, *A&A*, 322, 523
- . 2006, *MNRAS*, 368, 579, doi: [10.1111/j.1365-2966.2006.10121.x](https://doi.org/10.1111/j.1365-2966.2006.10121.x)
- . 2009a, *MNRAS*, 397, 1420, doi: [10.1111/j.1365-2966.2009.14893.x](https://doi.org/10.1111/j.1365-2966.2009.14893.x)
- . 2009b, *PhRvD*, 79, 123010, doi: [10.1103/PhysRevD.79.123010](https://doi.org/10.1103/PhysRevD.79.123010)
- Beechert, J., Lazar, H., Boggs, S. E., et al. 2022, *Nuclear Instruments and Methods in Physics Research A*, 1031, 166510, doi: [10.1016/j.nima.2022.166510](https://doi.org/10.1016/j.nima.2022.166510)

- Bogdanov, S., Deller, A. T., Miller-Jones, J. C. A., et al. 2018, *ApJ*, 856, 54, doi: [10.3847/1538-4357/aaeb9](https://doi.org/10.3847/1538-4357/aaeb9)
- Bruel, P. 2019, *A&A*, 622, A108, doi: [10.1051/0004-6361/201834555](https://doi.org/10.1051/0004-6361/201834555)
- Bruel, P., Burnett, T. H., Digel, S. W., et al. 2018, arXiv e-prints, arXiv:1810.11394, <https://arxiv.org/abs/1810.11394>
- Caballero, I., Pottschmidt, K., Marcu, D. M., et al. 2013, *ApJL*, 764, L23, doi: [10.1088/2041-8205/764/2/L23](https://doi.org/10.1088/2041-8205/764/2/L23)
- Cheng, K. S., & Ruderman, M. 1991, *ApJ*, 373, 187, doi: [10.1086/170036](https://doi.org/10.1086/170036)
- Chernyakova, M., Malyshev, D., Mc Keague, S., et al. 2020, *MNRAS*, 497, 648, doi: [10.1093/mnras/staa1876](https://doi.org/10.1093/mnras/staa1876)
- Coe, M. J., Reig, P., McBride, V. A., Galache, J. L., & Fabregat, J. 2006, *MNRAS*, 368, 447, doi: [10.1111/j.1365-2966.2006.10127.x](https://doi.org/10.1111/j.1365-2966.2006.10127.x)
- Coe, M. J., Okazaki, A. T., Steele, I. A., et al. 2019, *MNRAS*, 485, 1864, doi: [10.1093/mnras/stz515](https://doi.org/10.1093/mnras/stz515)
- de Angelis, A., Tatischeff, V., Grenier, I. A., et al. 2018, *Journal of High Energy Astrophysics*, 19, 1, doi: [10.1016/j.jheap.2018.07.001](https://doi.org/10.1016/j.jheap.2018.07.001)
- de Jager, O. C., Raubenheimer, B. C., & Swanepoel, J. W. H. 1989, *A&A*, 221, 180
- de Martino, D., Papitto, A., Belloni, T., et al. 2015, *MNRAS*, 454, 2190, doi: [10.1093/mnras/stv2109](https://doi.org/10.1093/mnras/stv2109)
- de Oña Wilhelmi, E., Papitto, A., Li, J., et al. 2016, *MNRAS*, 456, 2647, doi: [10.1093/mnras/stv2695](https://doi.org/10.1093/mnras/stv2695)
- Deeter, J. E., Boynton, P. E., & Pravdo, S. H. 1981, *ApJ*, 247, 1003, doi: [10.1086/159110](https://doi.org/10.1086/159110)
- Dubus, G. 2015, *Comptes Rendus Physique*, 16, 661, doi: [10.1016/j.crhy.2015.08.014](https://doi.org/10.1016/j.crhy.2015.08.014)
- Fang, K., Charles, E., & Blandford, R. D. 2020, *ApJL*, 889, L5, doi: [10.3847/2041-8213/ab62b8](https://doi.org/10.3847/2041-8213/ab62b8)
- Fermi-LAT collaboration. 2022, arXiv e-prints, arXiv:2201.11184, <https://arxiv.org/abs/2201.11184>
- Finger, M. H., Wilson, R. B., & Harmon, B. A. 1996, *ApJ*, 459, 288, doi: [10.1086/176892](https://doi.org/10.1086/176892)
- Harvey, M., Rulten, C. B., & Chadwick, P. M. 2022, *MNRAS*, 512, 1141, doi: [10.1093/mnras/stac375](https://doi.org/10.1093/mnras/stac375)
- Hobbs, G. B., Edwards, R. T., & Manchester, R. N. 2006, *MNRAS*, 369, 655, doi: [10.1111/j.1365-2966.2006.10302.x](https://doi.org/10.1111/j.1365-2966.2006.10302.x)
- Kerr, M. 2011, *ApJ*, 732, 38, doi: [10.1088/0004-637X/732/1/38](https://doi.org/10.1088/0004-637X/732/1/38)
- Kong, L. D., Zhang, S., Ji, L., et al. 2021, *ApJL*, 917, L38, doi: [10.3847/2041-8213/ac1ad3](https://doi.org/10.3847/2041-8213/ac1ad3)
- Kong, L.-D., Zhang, S., Ji, L., et al. 2022, *ApJ*, 932, 106, doi: [10.3847/1538-4357/ac6e66](https://doi.org/10.3847/1538-4357/ac6e66)
- Li, J., Torres, D. F., Liu, R.-Y., et al. 2020, *Nature Astronomy*, 4, 1177, doi: [10.1038/s41550-020-1164-6](https://doi.org/10.1038/s41550-020-1164-6)
- Li, J., Torres, D. F., Zhang, S., et al. 2012, *ApJ*, 761, 49, doi: [10.1088/0004-637X/761/1/49](https://doi.org/10.1088/0004-637X/761/1/49)
- Lundy, M. 2021, arXiv e-prints, arXiv:2108.09350, <https://arxiv.org/abs/2108.09350>
- Mandal, M., & Pal, S. 2022, *MNRAS*, 511, 1121, doi: [10.1093/mnras/stac111](https://doi.org/10.1093/mnras/stac111)
- Mattox, J. R., Bertsch, D. L., Chiang, J., et al. 1996, *ApJ*, 461, 396, doi: [10.1086/177068](https://doi.org/10.1086/177068)
- McEnery, J., van der Horst, A., Dominguez, A., et al. 2019, in *Bulletin of the American Astronomical Society*, Vol. 51, 245, <https://arxiv.org/abs/1907.07558>
- Orellana, M., Romero, G. E., Pellizza, L. J., & Vidrih, S. 2007, *A&A*, 465, 703, doi: [10.1051/0004-6361:20066238](https://doi.org/10.1051/0004-6361:20066238)
- Papitto, A., & Torres, D. F. 2015, *ApJ*, 807, 33, doi: [10.1088/0004-637X/807/1/33](https://doi.org/10.1088/0004-637X/807/1/33)
- Papitto, A., Torres, D. F., & Li, J. 2014, *MNRAS*, 438, 2105, doi: [10.1093/mnras/stt2336](https://doi.org/10.1093/mnras/stt2336)
- Papitto, A., Ferrigno, C., Bozzo, E., et al. 2013, *Nature*, 501, 517, doi: [10.1038/nature12470](https://doi.org/10.1038/nature12470)
- Papitto, A., Ambrosino, F., Stella, L., et al. 2019, *ApJ*, 882, 104, doi: [10.3847/1538-4357/ab2fdf](https://doi.org/10.3847/1538-4357/ab2fdf)
- Rasul, K., Chadwick, P. M., Graham, J. A., & Brown, A. M. 2019, *MNRAS*, 485, 2970, doi: [10.1093/mnras/stz559](https://doi.org/10.1093/mnras/stz559)
- Romero, G. E., Kaufman Bernadó, M. M., Combi, J. A., & Torres, D. F. 2001, *A&A*, 376, 599, doi: [10.1051/0004-6361:20011044](https://doi.org/10.1051/0004-6361:20011044)
- Rosenberg, F. D., Eyles, C. J., Skinner, G. K., & Willmore, A. P. 1975, *Nature*, 256, 628, doi: [10.1038/256628a0](https://doi.org/10.1038/256628a0)
- Sartore, N., Jourdain, E., & Roques, J. P. 2015, *ApJ*, 806, 193, doi: [10.1088/0004-637X/806/2/193](https://doi.org/10.1088/0004-637X/806/2/193)
- Sierpowska-Bartosik, A., & Torres, D. F. 2008, *Astroparticle Physics*, 30, 239, doi: [10.1016/j.astropartphys.2008.09.009](https://doi.org/10.1016/j.astropartphys.2008.09.009)

- Sinitsyna, V. G., & Sinitsyna, V. Y. 2019, in European Physical Journal Web of Conferences, Vol. 208, European Physical Journal Web of Conferences, 14008, doi: [10.1051/epjconf/201920814008](https://doi.org/10.1051/epjconf/201920814008)
- Smith, D. A., Bruel, P., Cognard, I., et al. 2019, ApJ, 871, 78, doi: [10.3847/1538-4357/aaf57d](https://doi.org/10.3847/1538-4357/aaf57d)
- Stappers, B. W., Archibald, A. M., Hessels, J. W. T., et al. 2014, ApJ, 790, 39, doi: [10.1088/0004-637X/790/1/39](https://doi.org/10.1088/0004-637X/790/1/39)
- Steele, I. A., Negueruela, I., Coe, M. J., & Roche, P. 1998, MNRAS, 297, L5, doi: [10.1046/j.1365-8711.1998.01593.x](https://doi.org/10.1046/j.1365-8711.1998.01593.x)
- Tavani, M., Bulgarelli, A., Piano, G., et al. 2009, Nature, 462, 620, doi: [10.1038/nature08578](https://doi.org/10.1038/nature08578)
- Torres, D. F., Ji, L., Li, J., et al. 2017, ApJ, 836, 68, doi: [10.3847/1538-4357/836/1/68](https://doi.org/10.3847/1538-4357/836/1/68)
- van den Eijnden, J., Degenaar, N., Russell, T. D., et al. 2018, Nature, 562, 233, doi: [10.1038/s41586-018-0524-1](https://doi.org/10.1038/s41586-018-0524-1)
- van den Eijnden, J., Degenaar, N., Wijnands, R., et al. 2020, The Astronomer's Telegram, 14193, 1
- Veledina, A., Nättilä, J., & Beloborodov, A. M. 2019, ApJ, 884, 144, doi: [10.3847/1538-4357/ab44c6](https://doi.org/10.3847/1538-4357/ab44c6)
- Wang, P. J., Kong, L. D., Zhang, S., et al. 2022, ApJ, 935, 125, doi: [10.3847/1538-4357/ac8230](https://doi.org/10.3847/1538-4357/ac8230)
- Weng, S.-S., Qian, L., Wang, B.-J., et al. 2022, Nature Astronomy, 6, 698, doi: [10.1038/s41550-022-01630-1](https://doi.org/10.1038/s41550-022-01630-1)
- Xing, Y., Wang, Z., Zhang, X., Chen, Y., & Jithesh, V. 2019, ApJ, 872, 25, doi: [10.3847/1538-4357/aafc60](https://doi.org/10.3847/1538-4357/aafc60)
- Zanin, R., Fernández-Barral, A., de Oña Wilhelmi, E., et al. 2016, A&A, 596, A55, doi: [10.1051/0004-6361/201628917](https://doi.org/10.1051/0004-6361/201628917)
- Zdziarski, A. A., Malyshev, D., Chernyakova, M., & Pooley, G. G. 2017, MNRAS, 471, 3657, doi: [10.1093/mnras/stx1846](https://doi.org/10.1093/mnras/stx1846)
- Zdziarski, A. A., Malyshev, D., Dubus, G., et al. 2018, MNRAS, 479, 4399, doi: [10.1093/mnras/sty1618](https://doi.org/10.1093/mnras/sty1618)

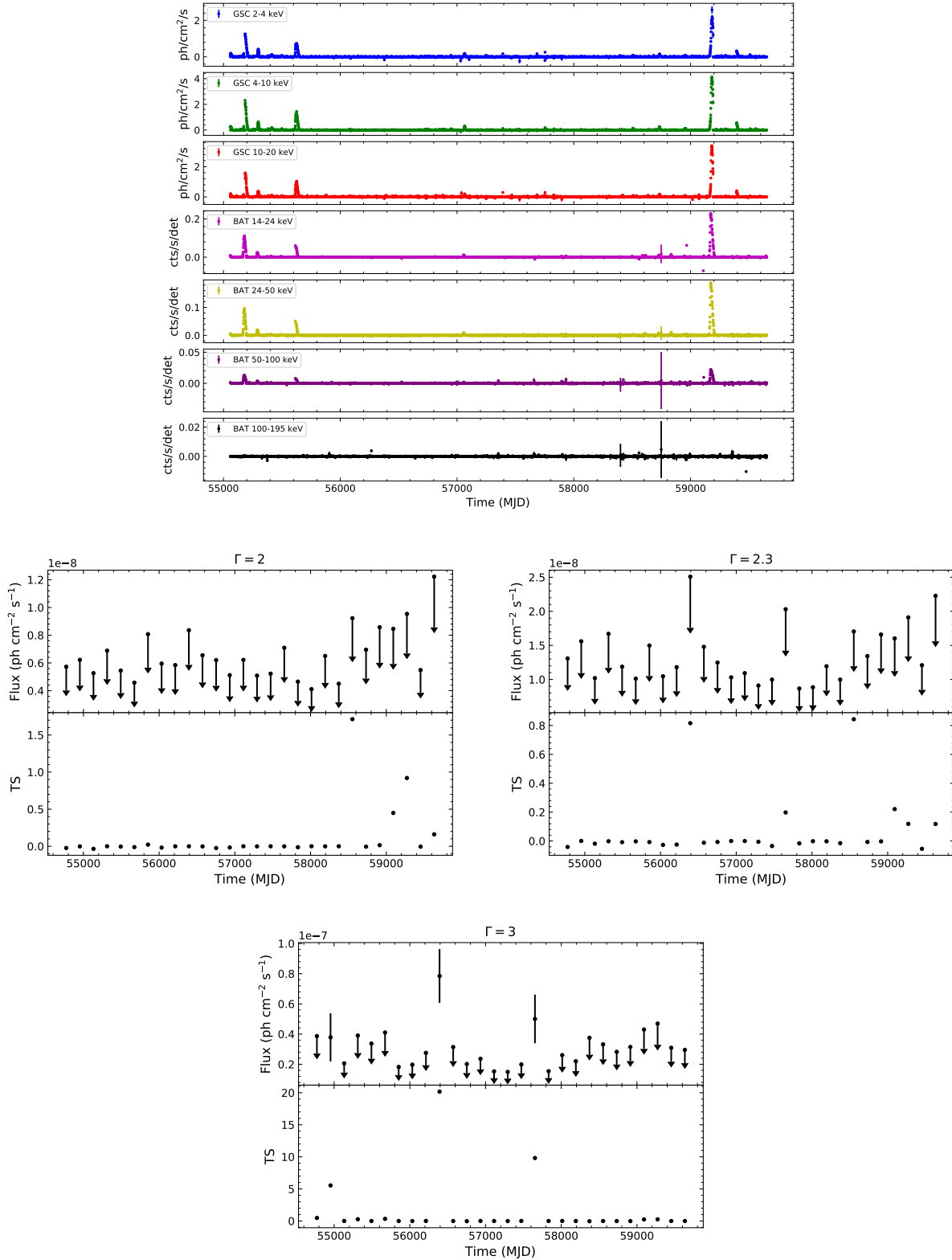


Figure 1. Upper panel: Long-term X-ray light curves of 1A 0535+262 in different energy bands observed by *Swift*/BAT and *MAXI*/GSC as obtained from http://sakamotoagu.mydns.jp/bat_gsc_trans_mon/web_lc/1_Day.php?name=1A_0535+262. Low three panels: Long-term gamma-ray light curves of 1A 0535+262 with a time binning of 180 days. Spectral index was fixed to 2, 2.3 and 3, respectively. Upper limits at 95% confidence level are computed for bins with $TS < 4$.

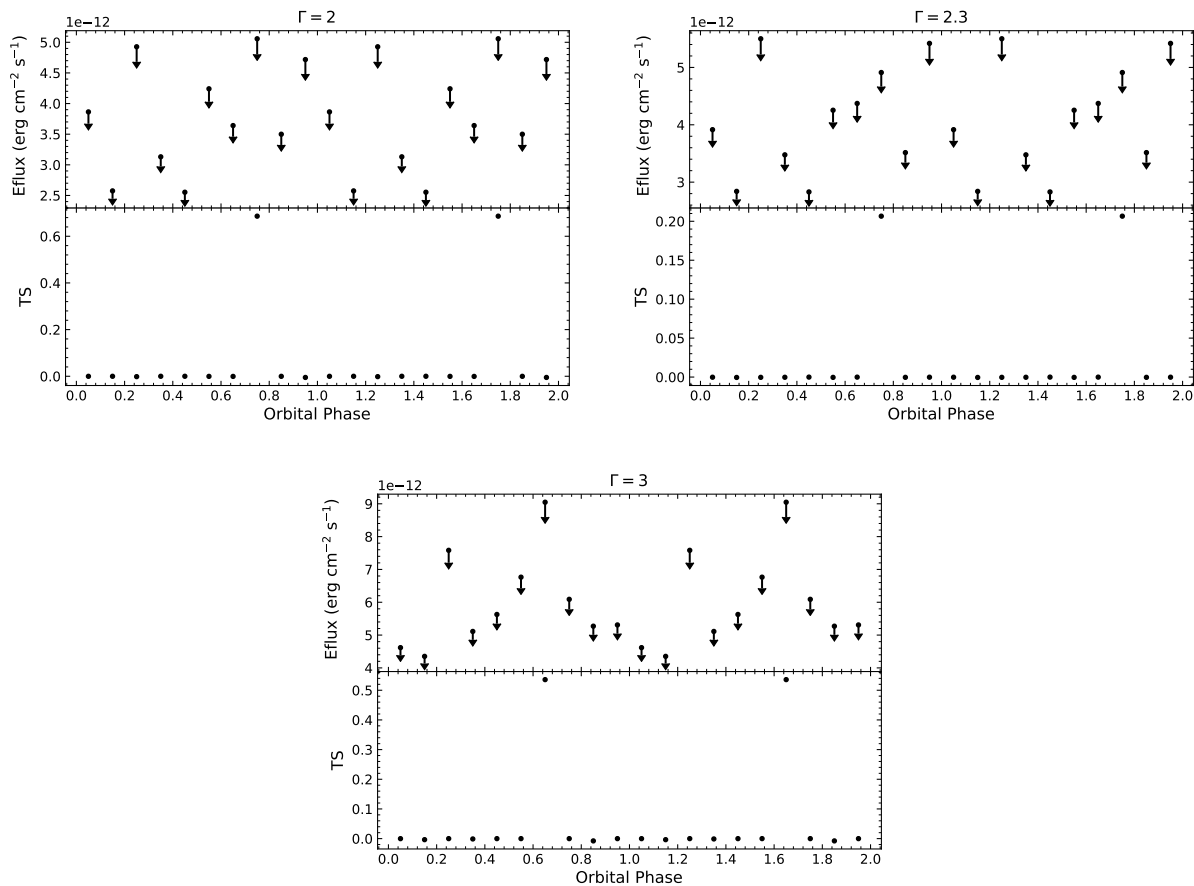


Figure 2. Orbital energy flux variation of 1A 0535+262 with 10 bins per orbit. Spectral index was fixed to 2, 2.3 and 3, respectively. Upper limits at 95% confidence level are computed for bins with $TS < 4$.

Table 1. *Fermi*-LAT spectral analysis results

Period ^a	Time Range (MJD)	Spectral Index	TS	Energy Flux Upper Limit ^b (10^{-12} erg cm ⁻² s ⁻¹)
Whole dataset				
full	54682-59739	2.0	0.0	0.6
full	54682-59739	2.3	0.0	0.7
full	54682-59739	3.0	0.0	1.2
Stacked outbursts				
Rising+Falling	55040-59207	2.0	0.0	11.9
Rising+Falling	55040-59207	2.3	0.0	9.3
Rising+Falling	55040-59207	3.0	0.0	20.9
The 2009 double-peaked outburst				
Rising+Falling	55040-55070	2.0	0.4	34.9
Rising+Falling	55040-55070	2.3	0.4	27.3
Rising+Falling	55040-55070	3.0	0.0	21.9
The 2009 giant outburst				
ALL	55165.9-55249.6	2.0	0.0	9.9
ALL	55165.9-55249.6	2.3	0.0	10.5
ALL	55165.9-55249.6	3.0	0.0	16.5
Rising+Falling	55165.9-55193.6	2.0	0.0	27.9
Rising+Falling	55165.9-55193.6	2.3	0.0	24.7
Rising+Falling	55165.9-55193.6	3.0	0.0	28.4
Rising	55165.9-55177.6	2.0	0.0	49.3
Rising	55165.9-55177.6	2.3	0.0	45.8
Rising	55165.9-55177.6	3.0	0.0	45.4
Falling	55178.4-55193.6	2.0	0.0	39.4
Falling	55178.4-55193.6	2.3	0.0	31.7
Falling	55178.4-55193.6	3.0	0.0	29.5
Apastron	55199.4-55216.6	2.0	0.0	23.6
Apastron	55199.4-55216.6	2.3	0.0	18.1
Apastron	55199.4-55216.6	3.0	0.0	18.6
Periastron	55230.4-55249.6	2.0	0.0	44.9
Periastron	55230.4-55249.6	2.3	0.0	39.3
Periastron	55230.4-55249.6	3.0	0.0	34.5
The 2011 giant outburst				
Rising+Falling	55600-55645	2.0	0.0	14.6
Rising+Falling	55600-55645	2.3	0.0	13.4
Rising+Falling	55600-55645	3.0	0.0	19.6
Rising	55600-55617	2.0	0.0	33.0
Rising	55600-55617	2.3	0.0	30.7
Rising	55600-55617	3.0	0.0	40.0
Falling	55618-55645	2.0	0.0	30.9
Falling	55618-55645	2.3	0.0	30.6
Falling	55618-55645	3.0	0.0	20.0
The 2020 giant outburst				
Rising+Falling	59159-59207	2.0	0.0	33.4
Rising+Falling	59159-59207	2.3	0.0	27.2
Rising+Falling	59159-59207	3.0	0.0	31.4
Rising	59159-59172.5	2.0	4.2	131.5
Rising	59159-59172.5	2.3	3.2	91.8
Rising	59159-59172.5	3.0	0.5	90.0
Falling	59173-59207	2.0	0.0	24.2
Falling	59173-59207	2.3	0.0	22.0
Falling	59173-59207	3.0	0.0	30.5

^a Full: the whole dataset used in this work; ALL: the dataset including the rising, falling, apastron and periastron portions of the outburst.

^b The upper limits are given at the 95% confidence level in the energy range of 0.1–300 GeV.

Table 2. Parameters of the spin evolution of 1A 0535+026. ν_i is the i th order derivative of the frequency.

Parameters	2009 double outburst ^a	2009 outburst ^a	2011 outburst ^b	2020 outburst ^c
Epoch (MJD)	55040	55166.99	55616.202	59170
T_{start} (MJD)	55040	55166.99	55608	59159.15
T_{stop} (MJD)	55070	55201	55637	59207.92
$\nu_0(10^{-3} \text{ Hz})$	9.66041(4)	9.6618(1)	9.6793(1)	9.66045(2)
$\nu_1(10^{-12} \text{ Hz s}^{-1})$	0.67(3)	-4.6(6)	6.43(5)	19.27(4)
$\nu_2(10^{-17} \text{ Hz s}^{-2})$		3.3(0.3)	0.121(7)	1.17(4)
$\nu_3(10^{-23} \text{ Hz s}^{-3})$		-4.8(6)	-1.43(9)	-5.8(2)
$\nu_4(10^{-29} \text{ Hz s}^{-4})$		3(1)	1.67(5)	-2.8(9)
$\nu_5(10^{-36} \text{ Hz s}^{-5})$		-8(6)		737(7)
$\nu_6(10^{-39} \text{ Hz s}^{-6})$				-1.6(2)
$\nu_7(10^{-45} \text{ Hz s}^{-6})$				-5(2)
$\nu_8(10^{-50} \text{ Hz s}^{-6})$				3(1)
$\nu_9(10^{-56} \text{ Hz s}^{-6})$				-8(2)
$\nu_{10}(10^{-62} \text{ Hz s}^{-6})$				7(1)

^a: Derived from the *Fermi*/GBM monitoring (see text).

^b: Adopted from Sartore et al. (2015).

^c: Derived from *Insight*-HXMT observations (Wang et al. 2022, see text).